

Küresel Bombeli Basıncılı Kap Analiz ve Tasarımı

Hasan Huseyin OZKAN¹, Safa OZHAN¹, Garip GENÇ²

¹Cimtas Pipe Fabrication and Trading Ltd. Co. R&D Center, Bursa Free Zone, Gemlik/Bursa, Turkey

²Marmara University, Technology Faculty, Mechatronics Engineering Department, Istanbul, Turkey

e-posta: ggenc@marmara.edu.tr

Geliş Tarihi:29.04.2019

; Kabul Tarihi:30.05.2019

Özet

Bu çalışmada küresel bombe merkezinde ve kaynaklı plaka ile takviyelenmiş bir nozul açıklığı iç basınç yüklemesi altında sonlu elemanlar yöntemiyle tasarım prosedürünü anlamak amacıyla incelenmiştir. Bu prosedür ASME Boiler and Pressure Vessel Code Section VIII Division 2 standardına göre ele alınmıştır. Bu standart ilki "Formüller ile Tasarım" ve ikincisi "Analiz ile Tasarım" olmak üzere basınçlı kap tasarımı için iki farklı kısım içerir. ASME standardı referans alınarak, "Plastik Çökme" ve "Lokal Hasar" hasar modlarına karşı dayanımı doğrulamak için aksisimetrik sonlu eleman modelleri ile elastik, limit yük ve elastik-plastik analiz yöntemleri kullanılmıştır. Maksimum izin verilen basınçlar bu analiz yöntemlerine göre elde edilmiş ve değerlendirilmiştir. Elastik ve limit yük analiz metodlarına göre elde edilen plastik çökme sonuçları birbirine çok yakındır. Bunun yanında plastik çökme hasar modu için elastik analiz yönteminin elastik-plastik analiz yöntemine göre daha konservatif sonuçlar verdiği gözlemlenmiştir. Diğer yandan, lokal hasar modu için elastik-plastik analiz yönteminin elastik analize göre nispeten konservatif olduğu gözlemlenmiştir.

Anahtar kelimeler

İç Basınca Maruz Basıncılı Kaplar; Sonlu Elemanlar Yöntemi; Formüller ile Tasarım; Analiz ile Tasarım

Analysis and Design of Hemispherical Head Pressure Vessel

Abstract

In this study, a hemispherical head with pad reinforced central nozzle opening that subjected to uniform internal pressure was investigated using Finite Element Methods (FEM) to understand the design procedure. This procedure is handled according to the ASME Boiler and Pressure Vessel Code Section VIII Division 2. This standard contains two parts for the design of pressure vessels, the first part is Design by rules and the second part is Design by analysis. With reference to the ASME standard, axisymmetric finite element models for Elastic, Limit Load and Elastic-Plastic Analysis are used to demonstrate protection against plastic collapse and local failure. Maximum allowable pressures are obtained in accordance with the mentioned design methods and discussed. According to the elastic and limit load analysis methods, obtained plastic collapse results are very close. Besides, the elastic analysis method is observed to be more conservative than the Elastic-Plastic method regarding the evaluation of plastic collapse. On the other hand, for the local failure results, Elastic-Plastic Analysis is observed to be slightly conservative than the Elastic Analysis.

Keywords

Internally Pressurized Pressure Vessels; Finite Element Method; Design by Rules; Design by Analysis

1 Introduction

The pressure vessels, which are subjected to internal or external pressure, are used to store fluids such as oil, petroleum, and chemical. The risks which depending on the usage places of pressure vessels make these structural elements

important engineering equipment. The failure of pressure vessels may cause serious damage; therefore, pressure vessel design criteria and design steps gain significance. ASME standards are widely used for the design of these kinds of tubes. When the literature is examined, many studies

have been done to design pressure vessels using ASME codes (Bhagyashri and Mishra, 2015; Dhalla and Jones, 1986; Sunil Kumar and Suhas, 2016; Thakkar and Thakkar, 2012). Also, valuable studies which focused on design parameters of pressure tubes (such as their geometries) are found in the literature. For example, Agrawal and Ganesh Narayanan (2018) studied on an analysis of pull-out tests of Mild Steel tube stainless sheet joint fabricated by tube end forming. They observed that the end formed joint fails by joint unlocking, while it is a physical failure in case of the welded structure. Olszewski et al. (2018) carried out the analysis, project, and experimental examination of an original rigid riser for Coil Tubing Pipes. According to the present conclusion in this study, the theoretical and experimental examination has shown that the designed riser meets all adopted design assumptions, which proves its serviceability. Sharifi et al. (2018) focused on the effect of dome geometrical shape such as hemispherical, torispherical, and ellipsoidal domes, on mechanical deformation and cracked length of laminated woven reinforced polymer composite pressure vessels under low-velocity impact and internal pressure. According to the presented results in this study, the maximum and the minimum crack lengths also take place in torispherical and hemispherical domes, respectively. In another study of Sharifi et al. (2016), strain deformation of three types of internally pressurized laminated composite shells (hemispherical, ellipsoidal, and torispherical) with two types of woven roving stacking sequence was carried out numerically and experimentally in this study. According to the presented results in this study, laminated hemispherical shells were also found to be the preferred choice against mechanical failure while laminated torispherical shells were found to be the least choice.

In this study, a hemispherical head with a pad reinforced nozzle opening subjected to the uniform internal pressure is designed in accordance with Part 4 requirements. Then, the same design is evaluated with Part 5 Design by

Analysis methods of (ASME, 2017c) in order to compare the different design methods provided by this ASME standard.

2 Material and Method

A finite element model is developed in order to apply the design by analysis methods. Details of the FEM model such as geometry, mesh modeling, boundary conditions, material properties are briefly explained. All applicable loads on the component shall be considered when performing a design-by-analysis. The load case definition shall be included in the User's Design Specification. For this problem, two load cases are evaluated. For the first load case, design pressure, 3.6 MPa, is considered at 300°C. The second load case is shutdown case at 20°C. It should be noted that the effects of deadweight and hydrostatic pressure are neglected.

2.1 Finite Element Model

The details of the finite element model are provided within this section. The same finite element model is used as elastic, limit-load, elastic-plastic analysis models except for that magnitude of the applied internal pressure, material properties and exclusion of the nonlinear geometric effects are defined in conjunction with the corresponding analysis method.

In this section, the development stages of the finite element model starting with the geometry basis to analysis is explained. Abaqus software is used for modeling, preprocessing and post-processing of the model.

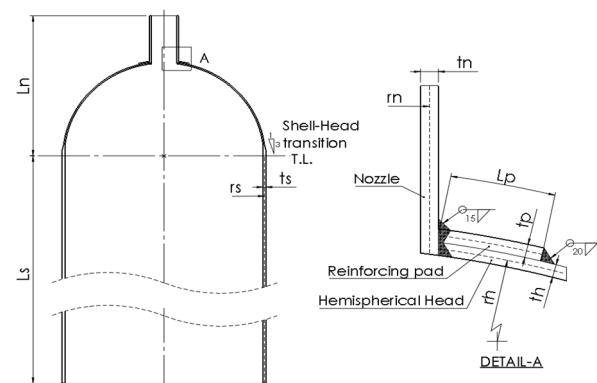


Figure 1. Geometry details basis to analysis

In Figure 1, the geometry and dimensional notation of the hemispherical head and the nozzle opening is shown. Values of these dimensions are also defined in Table 1.

Table 1. Dimensions of the model

Definition	Dimension [mm]
t_h : thickness of the hemispherical head	20
t_n : thickness of the nozzle	25.4
t_p : thickness of the reinforcing pad	20
t_s : thickness of the cylindrical shell	40
r_h : mean radius of the spherical shell	1420
r_n : mean radius of the round nozzle	190.5
r_s : mean radius of the cylindrical shell	1420
L_n : nozzle projection distance from the tangent line	2130
L_s : cylindrical shell length from the tangent	8000
L_p : width of the reinforcing pad	150

An axisymmetric finite element model is developed for this geometry. Axisymmetric elements provide for the modeling of the bodies of revolution under axially symmetric loading conditions. For this problem, the internal pressure loading and geometry is suitable for axisymmetric modeling. Axisymmetric elements are described in cylindrical polar coordinates r, z, θ denoted by 1, 2, 3 respectively. Cross-sectional model is developed in $\theta=0$. The radial and axial coordinates of a point on this cross-section are denoted by r and z , respectively. At $\theta=0$, the radial and axial coordinates coincide with the global Cartesian X and Y coordinates. The elements in this problem have following degree of freedoms; translations about Cartesian X (U1) and Cartesian Y (U2) directions and rotation about Cartesian Z direction (UR3) only.

Boundary conditions applied to the model are shown in Figure 2. Axial lengths of the cylindrical shell (L_s) and nozzle (L_n) are kept long enough in order to remove the effects of boundary conditions on the stress results obtained at the nozzle-head junction and shell head-transition regions. A hemispherical cap is modeled at nozzle end in order to involve the pressure thrust load acting on the junction.

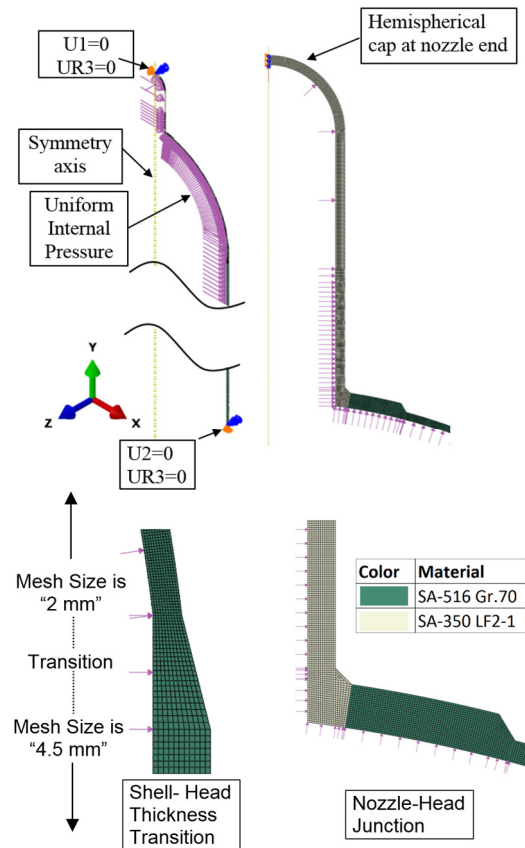


Figure 2. Finite Element Model

Materials assigned to the model regions are also shown in Figure 2. The material properties assigned to these material regions and applied internal pressures are given under corresponding design by analysis method. The reinforcing pad is assumed to be integral with the head. For the nozzle weld, considering the allowable stress of the materials, property of the weaker one of the connecting materials is assigned. Also, weld joint efficiency per (ASME, 2017c) is 1.0; therefore it is neglected in the evaluations.

CAX8R 8-node biquadratic, reduced integration axisymmetric solid elements used for mesh modeling. A global mesh size of “2 mm” for the regions above shell-head transition and a global mesh size of “4.5 mm” is used regions under the shell-head transition. The total number of elements used in the model is 37916, and average aspect ratio of all element is 1.16. The aspect ratio for all elements is less than 2.0.

2.2 Elastic Analysis Method

By the Elastic analysis method, protection against plastic collapse and local failure are demonstrated. Also, a ratcheting assessment is required even if the equipment is not in cyclic service.

An internal pressure load equal to the design pressure, 3.6 MPa, is applied to the pressure boundaries. Linear, elastic and isotropic material properties are utilized for this method. Considering the carbon content of the materials listed by (ASME, 2017a) and according to the Table TM-1 and Table PRD of (ASME, 2017b), assigned modulus of elasticity is 185000 MPa, and the Poisson’s ratio is 0.3 for both materials.

A static-stress displacement analysis is run neglecting the nonlinear geometric effects. Initial and deformed shapes of the model and the maximum stress location are shown in Figure 3.

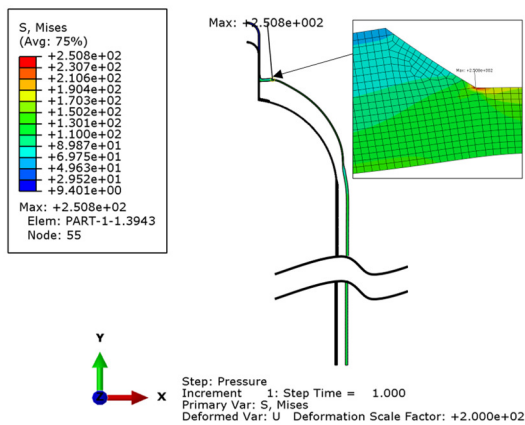


Figure 3. Elastic Nodal Averaged Stress and Displacement (x200 scaled) Results

As seen in Figure 3, the nozzle end is free only in the axial direction, and shell bottom edge is free only in the radial direction in accordance with the applied boundary conditions.

If a detailed stress analysis such as finite element analysis performed using a numerical method, the stress results typically provide a combination of P_L+P_b (at locations away from discontinuities) and P_L+P_b+Q+F (at structural discontinuities or stress concentrations) directly. In order to derive the membrane, bending and peak components of stress distribution, stress linearization shall be performed. There are several

options regarding the stress linearization procedure which are listed by (ASME, 2017c) and WRC429 (Hechmer and Hollinger, 1998). Structural stress method based on stress integration is recommended by (ASME, 2017c); this method is applied for stress linearization.

To produce valid membrane and bending stresses, there are some guidelines in Annex 5-A of (ASME, 2017c) for selecting the appropriate locations and orientations of SCLs. Regarding the orientation of the SCLs, the endpoints of the line should be chosen so that the section is normal to the interior and exterior surfaces of the model. This orientation minimizes problems with shear stresses since they will be approximately zero at the ends of the line (ASME, 2017c). Applied stress linearization lines along the model are shown in Figure 4.

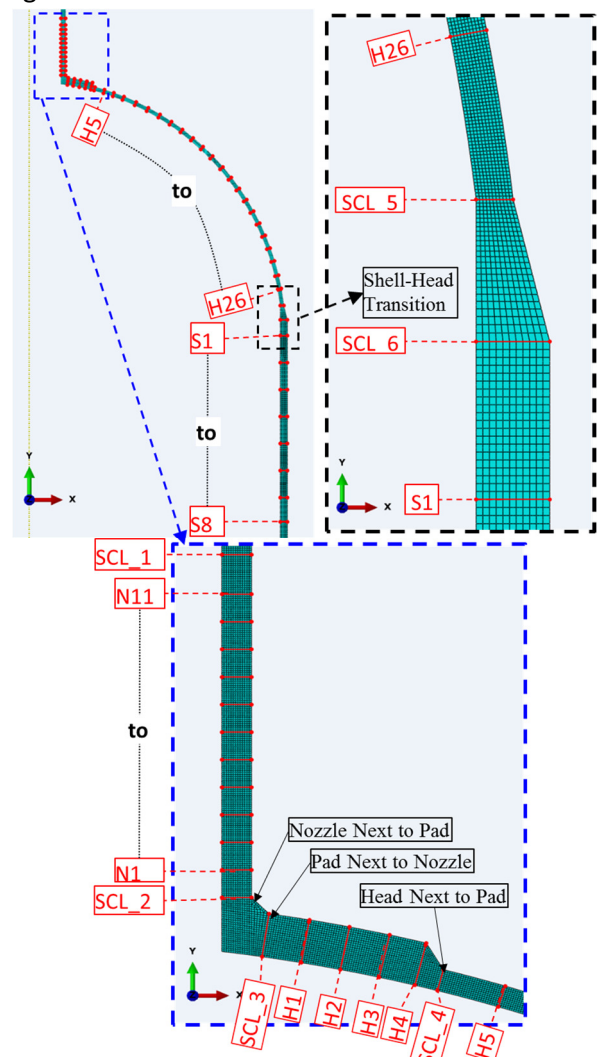


Figure 4. Stress Classification Lines (SCLs)

Obtained Von Mises equivalent linearized stresses and the allowable limits (S, SPL, SPS) along the model are depicted in Figure 5. The allowable limit “S” on general primary membrane equivalent stress (P_m), and the allowable limit “SPL” on local primary membrane (P_L) and primary general or local membrane plus primary bending equivalent stresses (P_L+P_b) are to be satisfied in order to demonstrate protection against plastic collapse. Secondary equivalent stress (Q) and additional equivalent stress produced by a stress concentration and above the nominal “P+Q” stress level (F) do not need to be determined to evaluate protection against plastic collapse. However, these equivalent stresses are needed to be evaluated for fatigue and ratcheting evaluations.

The allowable limits S, SPL and SPS on corresponding equivalent stresses are obtained in accordance with (ASME, 2017c). The hot (300°C) and cold (20°C) load cases are considered for the calculation of these allowable limits. Considering the internal pressure & hot loading case and cold & shutdown case, SPS is calculated in order to demonstrate protection against ratcheting.

Calculated values S, SPL, SPS parameters in accordance with (ASME, 2017c) are given in Table 2. The subscript “n” denotes for the nozzle and the material SA-350 Gr. LF-2 Cl.1, the subscript “s” denotes for head and shell and the material is SA-516 Gr.70.

Table 2. Values of S, SPL, SPS

Parameter	Value (MPa)
S_n	129
S_s	136
SPL_n	194
SPL_s	204
SPS_n	442.0
SPS_s	466.5

Computed linearized equivalent stresses along the SCLs depicted by Figure 4 and the allowable limits S, SPL, SPS for stress categories are demonstrated in Figure 5. For membrane plus bending, membrane plus bending plus peak equivalent stresses and the sum of principals are

calculated at inside and outside locations for each classification line, but only the governing of these values are plotted in Figure 5. Membrane equivalent stress obtained by “load controlled loads” are either classified as primary general or local membrane stress, i.e., P_m or P_L . Similarly, obtained membrane plus bending stresses are either classified as P_L+P_b for locations away from structural discontinuities or P_L+P_b+Q at local structural discontinuities.

Membrane equivalent stresses at structural discontinuities are classified as local primary membrane stress if the following rule of Part 5 of (ASME, 2017c) applies, A region of stress in a component is considered as local if the distance over which the equivalent stress exceeds $1.1S$ does not extend in the meridional direction more than $(r*t)^{0.5}$. This rule is also demonstrated in Figure 5, $(r*t)^{0.5}$ distances are marked for nozzle, head and shell locations. Bending stresses within structural discontinuities are evaluated as secondary.

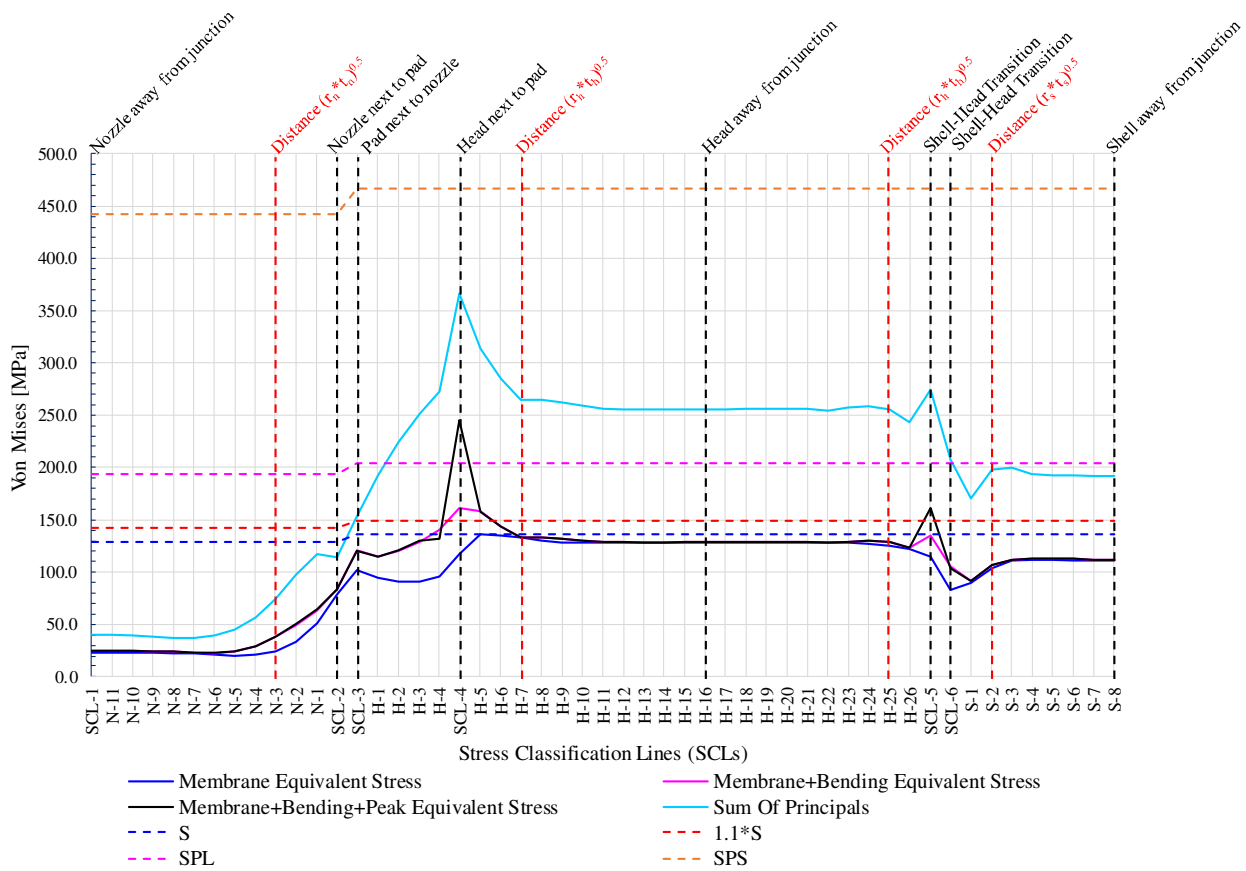


Figure 5. Distribution of the Linearized Equivalent Stresses along the Model

As seen in Figure 5, Membrane (P), membrane plus bending (P+B) and membrane plus bending plus peak (P+B+F) equivalent stresses are nearly coincident at the locations away from structural discontinuities, which shows the general membrane stress characteristics.

(P), (P+B) stresses are higher next to the nozzle-pad junction, pad-head and shell-head transition regions which are structural discontinuities. Especially for SCL-4 and SCL-5 (P+B+F) stresses are generated in excess of (P+B) stresses indicate the local stress concentration regions.

Table 3. Elastic Analysis Method: Protection against plastic collapse and ratcheting assessment

SCL	Definition	Membrane equivalent stress				Membrane plus bending equivalent stress			
		Category	Limit	Stress [MPa]	% Uti.	Category	Limit	Stress [MPa]	% Uti.
SCL-1	Nozzle away from junction	P_m	S_n	23.4	18.1	P_L+P_b	SPL_n	24.9	12.9
SCL-2	Nozzle next to pad	P_L	SPL_n	78.9	40.7	P_L+P_b+Q	SPS_n	83.6	18.9
SCL-3	Pad next to nozzle	P_L	SPL_s	101.9	50.0	P_L+P_b+Q	SPS_s	120.9	25.9
SCL-4	Head next to pad	P_L	SPL_s	117.4	57.6	P_L+P_b+Q	SPS_s	161.5	34.6
H-16	Head away from junction	P_m	S_s	127.8	94.0	P_L+P_b	SPL_s	128.7	63.1
SCL-5	Shell-Head Transition	P_L	SPL_s	115.2	56.5	P_L+P_b+Q	SPS_s	135.0	28.9
SCL-6	Shell-Head Transition	P_L	SPL_s	82.7	40.5	P_L+P_b+Q	SPS_s	105.4	22.6
S-8	Shell away from junction	P_m	S_s	110.6	81.3	P_L+P_b	SPL_s	112.2	55.0

Categorized stresses and comparison of these stresses to their corresponding allowable limits are summarized in Table 3. In Table 3, primary stress evaluations (P_m , P_L , and P_L+P_b) are satisfied to demonstrate the protection against

plastic collapse. The P_L+P_b+Q stress evaluations are for ratcheting assessment.

The protection against local failure is demonstrated in Table 4. It should be noted that

elastic local failure assessment uses only the primary membrane plus bending stresses.

Table 4. Elastic Analysis Method: Protection against local failure

SCL	Definition	Elastic Local Failure Criteria		
		Limit	Sum of Principals [MPa]	% Uti.
SCL-1	Nozzle away from the	$4S_n$	40.4	7.8
SCL-2	Nozzle next to pad	$4S_n$	113.6	22.0
SCL-3	Pad next to the nozzle	$4S_s$	153.4	28.2
SCL-4	Head next to pad	$4S_s$	366.2	67.3
H-16	Head away from the	$4S_s$	255.5	47.0
SCL-5	Shell-Head Transition	$4S_s$	274.0	50.4
SCL-6	Shell-Head Transition	$4S_s$	208.2	38.3
S-8	Shell away from the	$4S_s$	191.8	35.3

The protection against local failure may not be demonstrated if the design details are in accordance with Part 4 of (ASME, 2017c). However, all parts designed in accordance with Part 5 of (ASME, 2017c) shall be protected against local failure. In other words, protection against local failure shall be demonstrated for non-standard design details.

2.3 Limit Load Analysis

For the limit load analysis (LLA), elastic-perfectly plastic (no strain hardening behavior) material models are utilized as shown in Figure 6. $1.5 \cdot S$ yield strength is assigned for each of the materials in construction. The small-displacement theory is used for analysis; in other words, nonlinear geometric effects are not considered. This is mainly due to that pressure loading causes the structures to stiffen, and LLA method is not recommended for the cases which stiffness of the structure reduces by the applied loading.

LLA is essentially an alternative to the elastic analysis to perform protection against plastic collapse to limit the primary stresses. For the

internal pressure loading, the load factor to apply is 1.5 in accordance with (ASME, 2017c).

The pressure load causes the solver to diverge is the lower bound limit load of the structure. The equilibrium conditions are not satisfied for a small increase in the load, i.e., if the yield strength is reached over an entire cross-section, calculated displacements are infinite since the tangent modulus is zero.

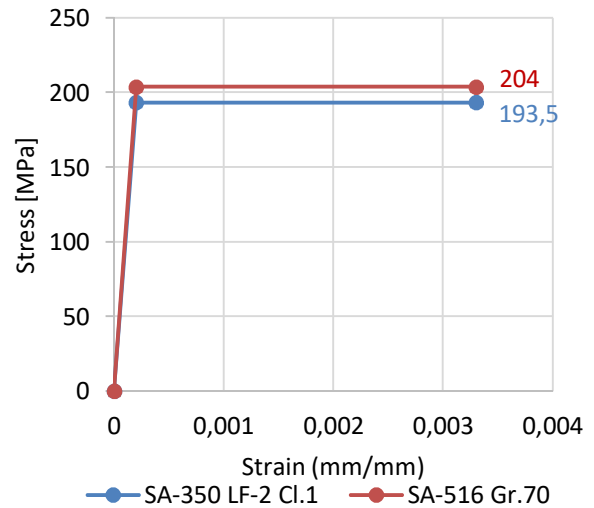


Figure 6. Limit Load Analysis: Material Models

In order to determine the limit load, ten times the design pressure, 36 MPa, is applied to the structure. Considering the minimum required limit load, the plastic collapse utilization is calculated as the 1.5 times the design pressure divided by the determined limit load. Protection against plastic collapse by LLA method is demonstrated as shown in Table 5.

Table 5. Limit Load Analysis Method: Plastic Collapse Utilization

Design Pressure (MPa)	Min Req'd (MPa)	Diverged Pressure (MPa)	Plastic Collapse % Utilization
3.6	5.4	5.75	93.9

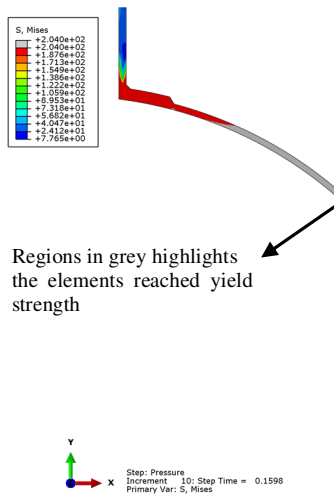


Figure 7. Limit Load Analysis: Divergence location

The region shown in grey in Figure 7 denotes the elements reached the yield strength at collapse pressure. The figure indicates that the head fails due to the general membrane stress.

2.4 Elastic-Plastic Analysis

Elastic-Plastic analysis method is utilized to demonstrate protection against plastic collapse, local failure, and ratcheting. For plastic collapse and local failure evaluation, the isotropic elastic-plastic material behavior involving strain hardening is used by the rules provided in Annex 3-D of (ASME, 2017c) and recommendations in (Peters et al. 2013). The strain of the proportional limit for the elastic-plastic material curves 1E-8. At that limit, true plastic strain is zero. Beyond the true ultimate stress, perfectly plastic material behavior is considered.

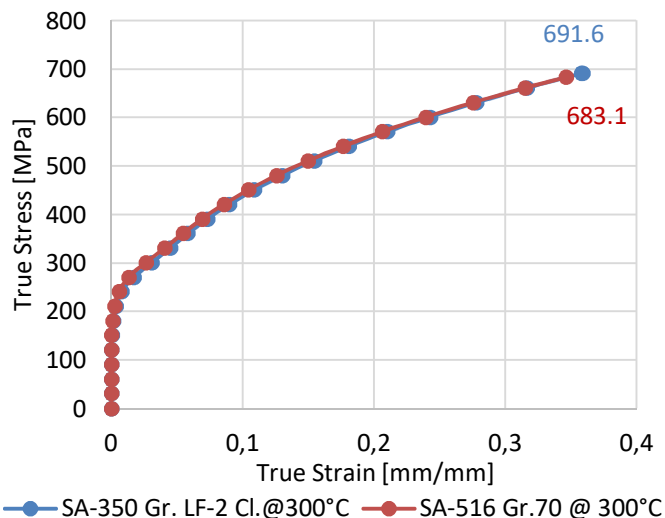


Figure 8. Elastic-Plastic Analysis: True Stress-Strain Curves

Table 6. Elastic-Plastic Analysis Method: Plastic Collapse Utilization

Design Pressure (MPa)	Min Req'd (MPa)	Diverged Pressure (MPa)	Plastic Collapse % Utilization
3.6	8.64	12.33	70.1

The pressure load factor for an elastic-plastic analysis is 2.4, which gives the minimum required pressure to be demonstrated for protection against plastic collapse. The diverged pressure column in Table 6 indicates that the internal pressure load causes the overall structural instability. The ratio of the minimum required collapse pressure, and the diverged pressure gives the plastic collapse utilization per the elastic-plastic analysis method.

In Figure 9, plastic strain distribution at plastic collapse pressure is shown. The elements in grey show the region has reached the plastic strain at true ultimate stress which shows the plastic collapse location.

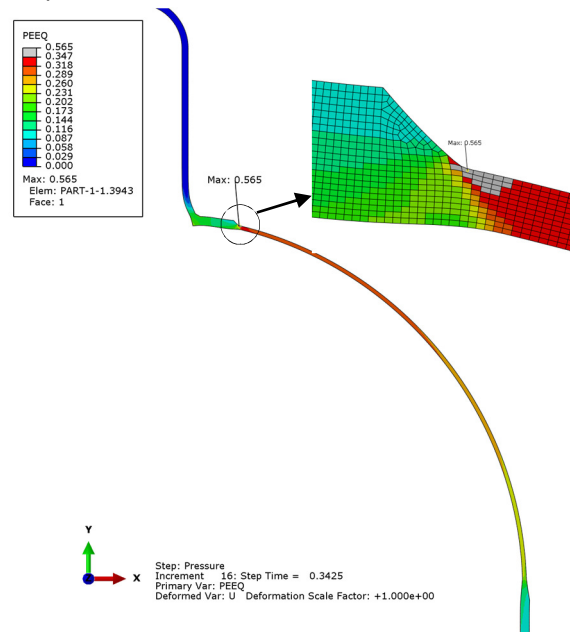


Figure 9. Elastic-Plastic Analysis: Plastic Strain distribution at collapse load

For protection against local failure, strain damage parameter is calculated at gauss points and extrapolated to the nodes for each element. For calculating the strain damage parameter (SLDR), the following are defined in the postprocessor in accordance with (ASME, 2017c).

$(\epsilon_{peq} + \epsilon_{cf}) \leq \epsilon_L$ where,

$$\epsilon_L = \epsilon_{Lu} \cdot \exp \left[- \left(\frac{\alpha_{sl}}{1 + m_2} \right) \left(\left\{ \frac{\sigma_1 + \sigma_2 + \sigma_3}{3\sigma_e} \right\} - \frac{1}{3} \right) \right] \quad Eq. 1$$

ϵ_L : limiting triaxial strain

$\sigma_1, \sigma_2, \sigma_3$: Principal stress components for each point in component

σ_e : Von Mises stress

α_{sl} : 2.2

$m_2 = 0.6 * (1 - R)$, where R is the ratio of yield and ultimate tensile strengths of the material

$\epsilon_{Lu} = m_2$

ϵ_{peq} : total equivalent plastic strain

ϵ_L : limiting triaxial strain

ϵ_{cf} : cold forming strain, assumed to be zero

$\left\{ \frac{\sigma_1 + \sigma_2 + \sigma_3}{3\sigma_e} \right\}$ stands for stress triaxiality.

$$SLDR = \frac{(\epsilon_{peq} + \epsilon_{cf})}{\epsilon_L} \leq 1.0 \quad Eq. 2$$

The load factor recommended for the elastic-plastic local failure evaluation is 1.7 per (ASME, 2017c). Figure 10 shows the computed local failure ratio at 1.7 times the design pressure. Calculating the strain damage parameter and satisfying the Eq. 2 per the required load cases is sufficient for demonstrating protection against local failure. However, for the purpose of this paper, the limit pressure for the elastic-plastic local failure is also obtained.

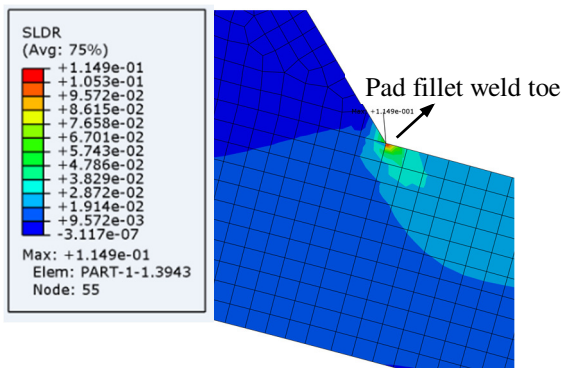


Figure 10. Elastic-Plastic Analysis: Maximum Strain Limit Damage Ratio (SLDR) Location at 6.12 MPa

The SLDR is computed for all the nodes in the model; Figure 10 shows its maximum location.

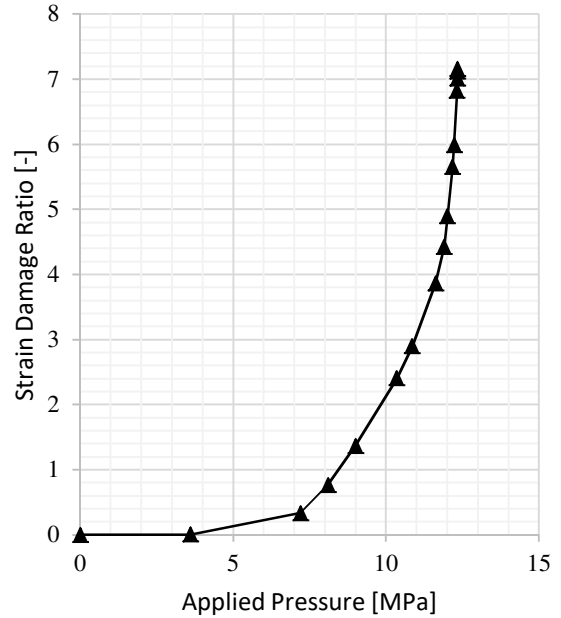


Figure 11. Elastic-Plastic Analysis: Strain Damage Parameters vs Pressure

The pressure load at which strain damage parameter is 1.0 is roughly obtained by calculating the parameter with increasing pressure loading as shown in Figure 11. According to that evaluation, the limiting pressure for local failure evaluation is estimated as 8.4 MPa.

An elastic-plastic ratcheting assessment is also performed. For this evaluation, the design pressure is applied to the model, and elastic-perfectly plastic material behavior is utilized with the Von Mises yield function and flow rule. Also, the effects of non-linear geometry are considered in the analysis. Three pressure cycles are applied to the model as a minimum required several cycles by (ASME, 2017c).

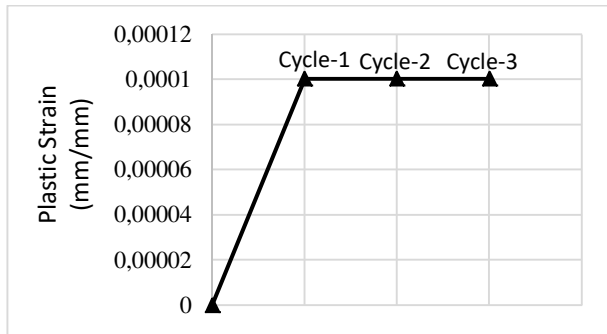


Figure 12. Elastic-Plastic Analysis Method: Ratcheting Assessment, Plastic Strain by Pressure Cycles

As shown in Figure 12, the magnitude of plastic strain does not propagate by pressure cycling; therefore, protection against ratcheting is demonstrated.

2.5 Part 4, Design By Rule Evaluation

For design by rule evaluation in accordance with Part 4 of (ASME, 2017c), only the maximum allowable pressure results are provided as given in Table 7.

Table 7. The maximum allowable pressure computed by Design by Rule requirements

Component	Design Pressure (MPa)	Design Temp. (°C)	Maximum Allowable Pressure (MPa)
Head	3.6	300	3.831
Cylinder	3.6	300	3.824
Nozzle	3.6	300	3.814

3 Results

The protection against plastic collapse and local failure are demonstrated by elastic, limit load and elastic-plastic design by analysis (DBA) methods. Also, ratcheting is assessed by Elastic and Elastic-Plastic analysis methods.

Table 8. Obtained Maximum Allowable Pressure by each Design Method

Design Method	Plastic Collapse % Uti.	Local Failure % Uti.	Maximum Allowable Pressure (MPa)
Elastic Analysis	94.0	67.3	3.83
Limit Load Analysis	93.9	67.3*	3.84
Elastic-Plastic Analysis	70.1	72.9	4.94
Design by Rule	-	-	3.814

(*): Local failure criteria check for a limit-load analysis is same

as elastic analysis.

The utilization of the applied design pressure and the maximum allowable pressures obtained by each of the design by analysis methods and the design by rule requirements are tabulated in Table 8.

4 Conclusion

According to the elastic and limit load analysis methods, obtained plastic collapse results are very close. Besides, the elastic analysis method is observed to be more conservative than the Elastic-Plastic method regarding the evaluation of plastic collapse. On the other hand, for the local failure results, Elastic-Plastic Analysis is observed to be slightly conservative than the Elastic Analysis. It should be noted that all three methods may be used to qualify a component in accordance with (ASME, 2017c), however, the elastic-plastic method is the most realistic DBA regarding the more realistic material input and included nonlinear geometric effects in the analysis.

The stress linearization and categorization processes for an elastic analysis are more complex compared to the post-processing of other methods and require more effort. Also, it may produce non-conservative results for thick walled ($R/t \leq 4$) pressure vessels. However, preprocessing and solver time for an elastic analysis are lesser compared to the other methods.

Limit load analysis method is shown to be excellent for demonstrating the protection against plastic collapse and may be used for general component sizing. However, similar to the elastic analysis, nonlinear geometric effects are excluded, and the buckling failure mode is not detected by this analysis method.

Predicted plastic collapse load in accordance with the elastic-plastic analysis method is considerably higher compared to the other analysis methods given the involved strain hardening behavior of the ductile material and applied pressure load factor.

Acknowledgment

This research is supported by Cimtas Pipe Fabrication and Trading Ltd. Co. with project number 9208-34.

5 References

- Agrawal, A. K., and Ganesh Narayanan, R., 2018. Pull-out tests on tube to sheet joints fabricated by endforming. *Journal of Constructional Steel Research*, 144, 186-197. doi:10.1016/j.jcsr.2018.01.027
- ASME. 2017a. Boiler and Pressure Vessel Code, Section II: Materials - Part A: Ferrous Material Specifications. In (Vol. ASME BPVC.II.A-2017): ASME International.
- ASME. 2017b. Boiler and Pressure Vessel Code, Section II: Materials - Part D: Properties. In (Vol. ASME BPVC.II.D.C-2017): ASME International.
- ASME. 2017c. Boiler and Pressure Vessel Code, Section VIII, Division 2: Alternative Rules. In (Vol. ASME BPVC.VIII.2-2017): ASME International.
- Bhagyashri, U., and Mishra, H., 2015. A review on design and analysis of pressure vessel. *International Journal of Advance Research and Innovative Ideas in Education*, 1(2), 348-353.
- Dhalla, A. K., and Jones, G. L., 1986. ASME code classification of pipe stresses: A simplified elastic procedure. *International Journal of Pressure Vessels and Piping*, 26(2), 145-166. doi:https://doi.org/10.1016/0308-0161(86)90038-4
- Hechmer, J. L., and Hollinger, G. L. (1998). 3D Stress Criteria Guidelines for Application. In *Welding Research Council Bulletin* (Vol. WRC - Bulletin 429): Welding Research Council.
- Olszewski, A., Wodtke, M., and Wójcikowski, A., 2018. FEM Analysis and Experimental Tests of Rigid Riser Hanging System. *Polish Maritime Research*, 25(2), 108-115. doi:10.2478/pomr-2018-0061
- Peters, D. T., Haley, K., and Padmala, A. (2013). *ASME Section VIII-Division 3 Example Problem Manual*.
- Sharifi, S., Gohari, S., Sharifiteshnizi, M., Alebrahim, R., Burvill, C., Yahya, Y., and Vrcelj, Z., 2018. Fracture of laminated woven GFRP composite pressure vessels under combined low-velocity impact and internal pressure. *Archives of Civil and Mechanical Engineering*, 18(4), 1715-1728. doi:10.1016/j.acme.2018.07.006
- Sharifi, S., Gohari, S., Sharifiteshnizi, M., and Vrcelj, Z., 2016. Numerical and experimental study on mechanical strength of internally pressurized laminated woven composite shells incorporated with surface-bounded sensors. *Composites Part B: Engineering*, 94, 224-237. doi:10.1016/j.compositesb.2016.03.020
- Sunil Kumar, D., and Suhas, B., 2016. Design and Evaluation of Pressure Vessel as per ASME Section VIII Division 2. *International Journal of Innovative Research in Science, Engineering and Technology*, 5(10), 17989-18002.
- Thakkar, B. S., and Thakkar, S. A., 2012. Design of Pressure Vessel Using ASME Code, Section VIII, Division 1. *International Journal of Advanced Engineering Research and Studies*, 1(2), 228-234.